



D.T3.1.1. Raw materials distribution models (RADM) for the 3 PMSD

June 2023

Isunza Manrique, I.¹, Kessouri, P.², Dumont, M.¹
Caterina, D.¹, Nguyen, F.¹

¹ULiège & ²BRGM



Summary

Summary	3
1. Introduction	4
2. WP Investment site n°1: Teesside (Uk)	6
2.1. Teesside site presentation.....	6
2.2. Field data processing methodology.....	7
2.3. Raw materials distribution model.....	8
3. Investment site n°2: Pompey (Fr)	10
3.1. Pompey site presentation.....	10
Site description.....	10
Geophysical field acquisition	10
Targeted sampling	11
Geochemical laboratory analyses.....	11
3.2. Methodology for data interpretation.....	12
3.3. Raw materials and pollution distribution model	12
Step 1: Creation of the field/lab dataset	12
Step 2: Geostatistical identification of correlations	12
Step 3: Definition of clusters	12
Step 4: field scale probabilistic classification.....	13
4. Investment site n°3: Duferco (Be)	16
4.1. Duferco site presentation	16
Site description.....	16
Geophysical field acquisition and targeted sampling.....	16
Geophysical laboratory measurements and geochemical analyses	17
4.2. Methodology for data interpretation.....	18
4.3. Raw materials distribution model.....	19
Preliminary conclusions	21
5. General conclusions	22

1. Introduction

The NWE-REGENERATIS project aims to develop new approaches to characterize past metallurgical sites and deposits (PMSD) by combining field geophysical measurements with geochemical and geophysical analyses of samples. Figure 1 presents the methodology workflow applied to build the RADMs of the project sites. The objective is first to provide a characterization of the site with geophysical field measurements. This characterization is used to define the location of the samples. These samples are positioned in order to validate the geophysical interpretations with direct field data. They are therefore positioned in sectors with varied geophysical properties. The geochemical measurements then allow the identification of the composition of the samples to be compared with the geophysical results.

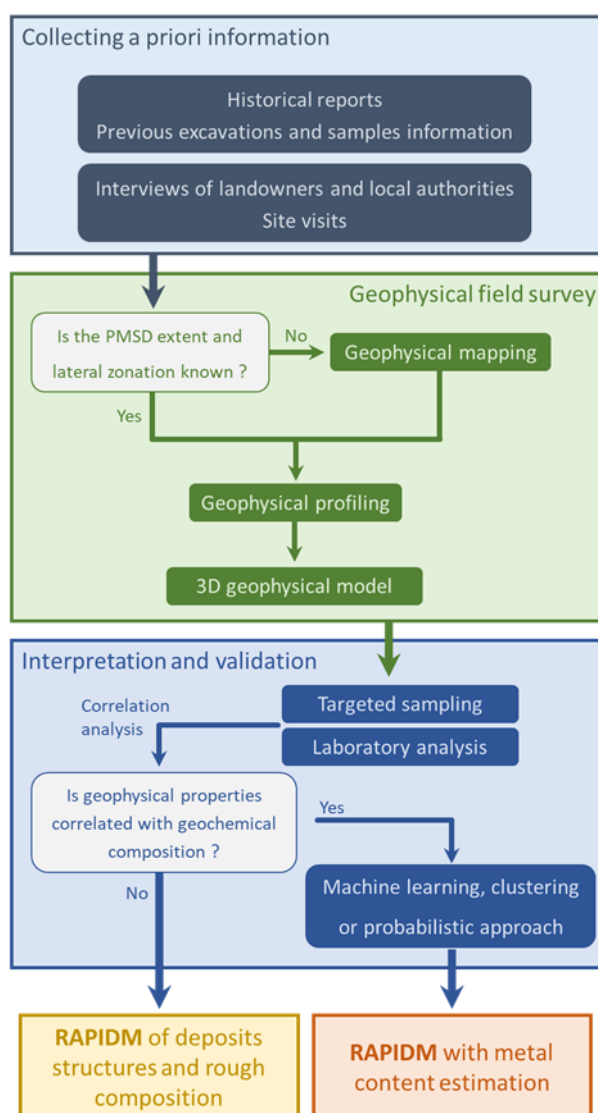


Figure 1 - Main steps of the suggested workflow on how to use geophysical techniques to build a RADM.

To improve this comparison, geophysical measurements can be made directly on the samples in order to limit the errors related to the difference in scale of geochemical and

geophysical measurements in the field. From these different measurements, a RADM can be built using statistical processing tools.

The purpose of this report is to present the stages of RADM construction for each of the investment sites: (1) Teesside in England; (ii) Pompey in France; and (iii) Duferco in Belgium. For each site, the historical, geophysical and geochemical data available or acquired are first summarized. For more information, the reader can refer to the project deliverables on site characteristics [D.I.1/2/3.1.1]; geophysical surveys [D.I.1/2/3.2.1]; and sampling investigations [D.I.1/2/3.2.2]. Then, the methodology developed for each site is presented in order to detail the results and extract the necessary information for the regeneration of the site.

2. WP Investment site n°1: Teesside (Uk)

2.1. Teesside site presentation

The South Tees Development Corporation [STDC] site is a large site (1500 ha) with a 160-year history of iron and steel production and the processing of finished products. The site has been used, at varying periods, for the storage of feedstock, products, by-products, and waste streams. The specific site selected for NWE-REGENERATIS project is called CLE31. It is mostly comprised of deposited slag materials, though various pieces of scrap materials were also noted. Vegetation growth existed in some areas within the CLE31 zone. Whilst much of the zone was flat and accessible, there were some piles and evidence that the deposits were not fully secure, likely due to the layers of the slag and air pockets as a result.

In May 2002, the BRGM and ULiege team used several methods during the geophysical survey:

- 3 mapping methods: electromagnetic induction, magnetic and magnetic susceptibility;
- 2 profiling methods: electrical resistivity and induced polarization tomographies.
- 17 soil samples were collected in the first centimeters of the landfill.

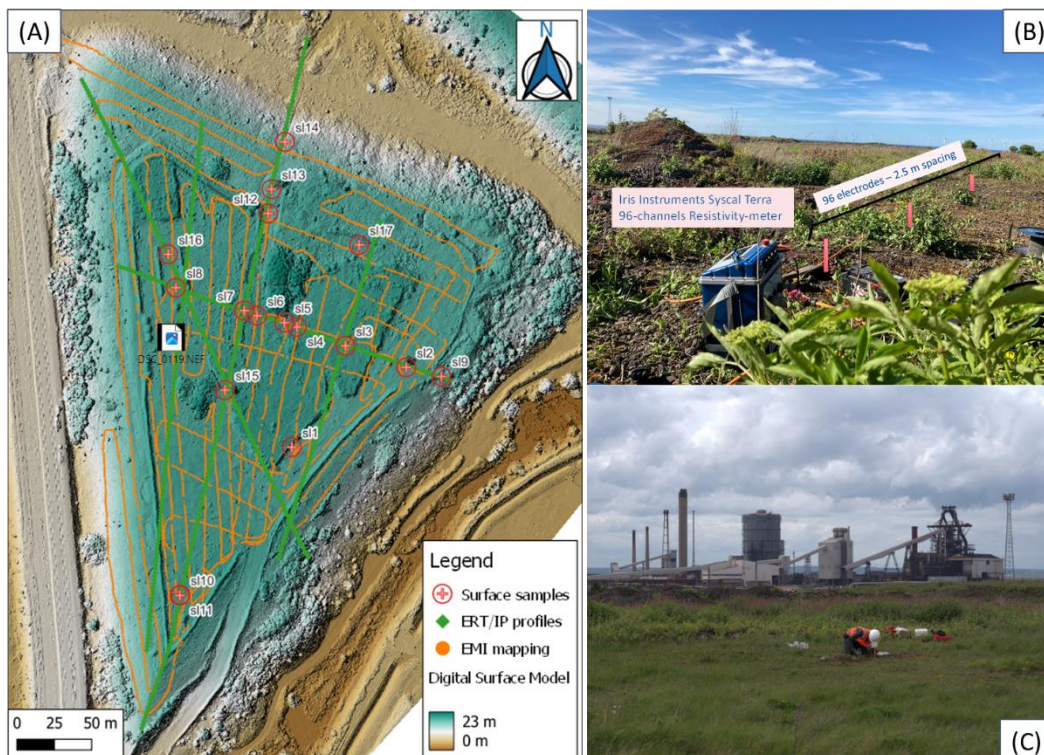


Figure 2: (A) Map of the site with EMI, ERT and IP geophysical acquisitions and the sampling locations. (B) photograph of the ERT/IP instrument in the field. (C) surface sampling in CLE31 site.

This first sampling survey was conducted in order to have first ideas of the geochemistry of the deposits, while waiting for a more extensive sampling survey. All the geophysical methods, except the magnetic susceptibility measurements have limited sensitivity at the surface, and up to a few centimeters, of the ground. Deeper samples, collected through drilling, would thus be more interesting to compare to the geophysical datasets. However, due to time and environmental issues, the drilling survey to provide deeper samples could not take place during the time of the NWE-REGENERATIS project. The geophysical interpretations available at Teesside CLE31 site are thus limited to qualitative ones. The geophysical dataset will only be analyzed as resistive/conductive and more or less chargeable layers. At the end, we propose interpretation which need to stay hypothetical without any deeper ground truth.

2.2. Field data processing methodology

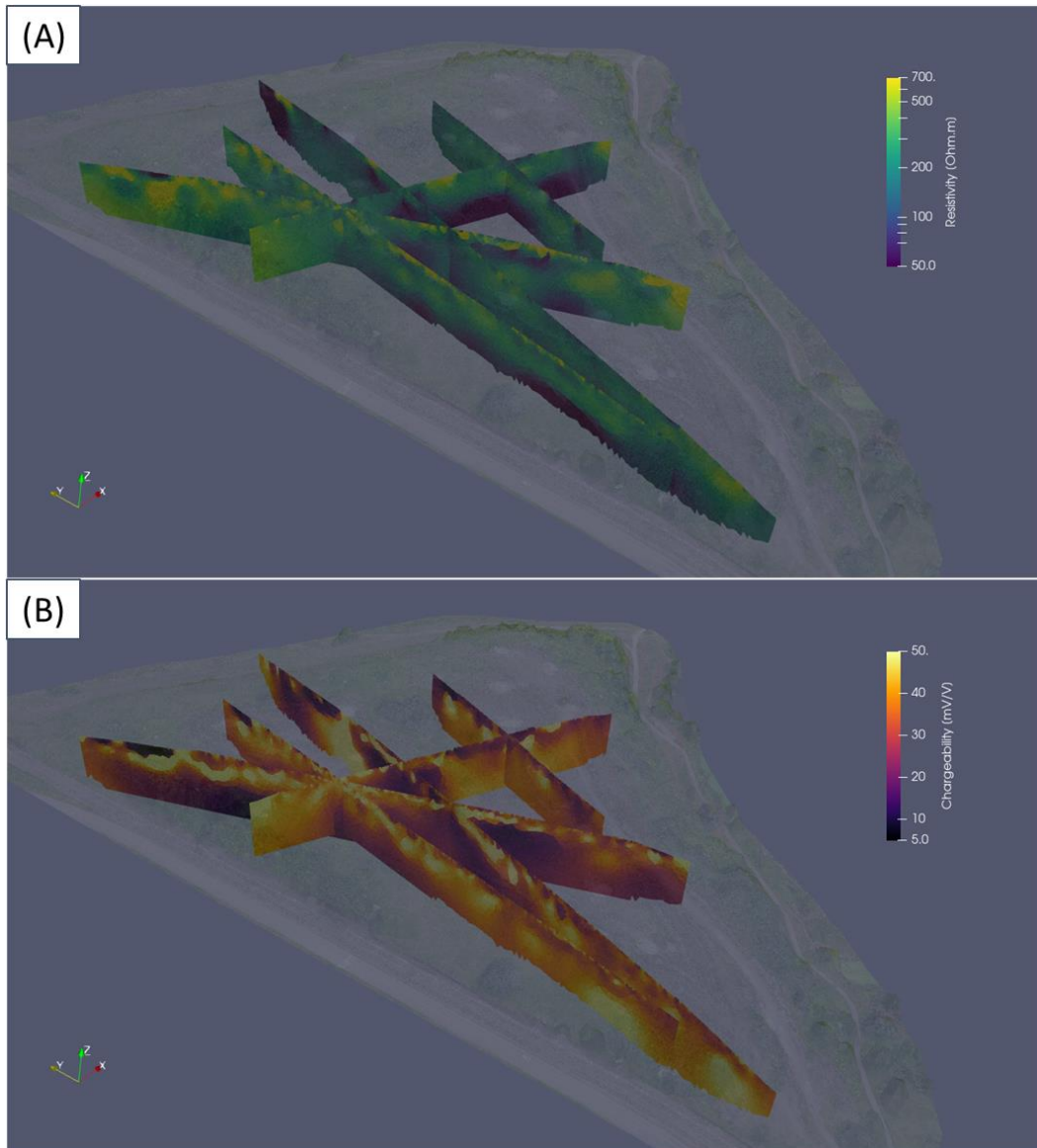


Figure 3: 3D view of the 5 resistivity (A) and chargeability (B) profiles covered by the digital surface model.

After the survey, several processing scheme of EMI data has been tested. They unveil the limit of the method on this site. The in-phase signal, partially linked to magnetic susceptibility, is highly variable and the apparent conductivity is negative in several areas. According to that, only qualitative interpretations have been proposed in the report DI1.2.1. Here, we then focus on ERT and IP models as they appear to be the more reliable measurement on this site.

After the standard analysis of ERT/IP data (filtering + error modelling), the datasets have been inverted in 2D using pyGIMLI software. This inversion provide a resistivity and chargeability 2D model for all profiles (Figure 3).

The resistivity and chargeability data estimated are then combined in a unique dataset. An agglomerative hierarchical clustering is used on the combined datasets to define clusters. The clusters gather closest data point in the resistivity / chargeability space (Figure 4).

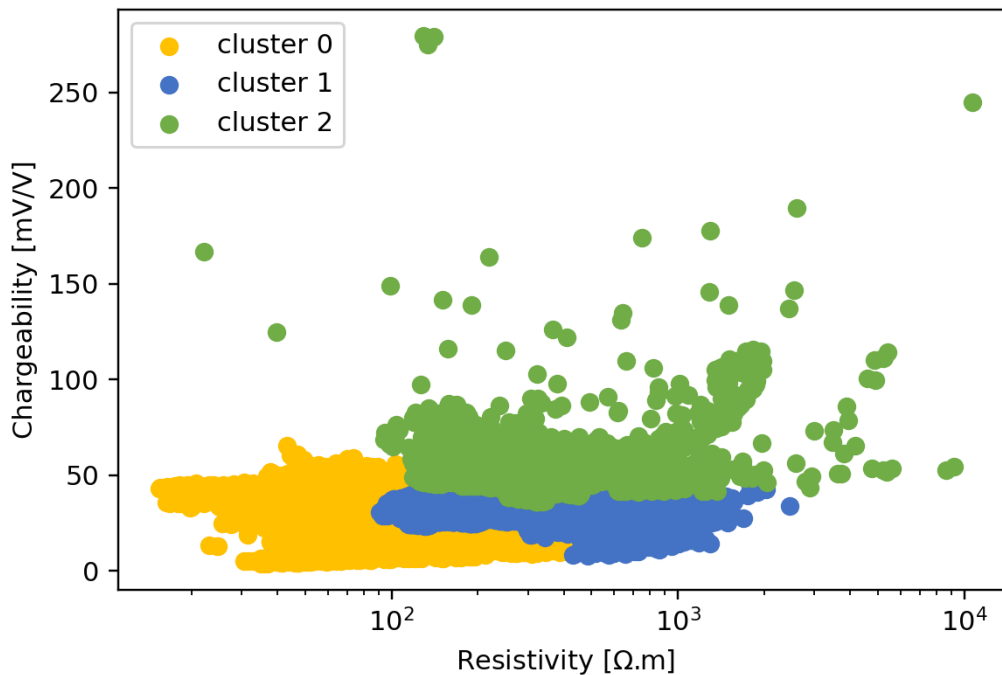


Figure 4: 3 clusters in the resistivity / chargeability space.

2.3. Raw materials distribution model

Thanks to the clustering approach, we obtain three clusters which can be represented in 3D (Figure 5).

The cluster n°0 (in yellow) is characterized by lower resistivity and chargeability. This cluster is mainly localized in the bottom part of the profiles and at the northern part of the site, characterized by more vegetation. According to these elements, this cluster might be related with natural ground and/or human limons/clay deposits to stabilize and/or divide the landfill.

The cluster n°1 (in blue) is characterized by higher resistivity and low chargeability. Localize above the cluster one it is the main component of the land slide. Cluster n°2 (in green) is characterized by the same high resistivity but with larger chargeability. Cluster n°2 is mainly embedded within the cluster n°1. According to these characteristics, we could consider that cluster n°1 (in blue) is related to anthropogenic deposits with low chargeable components. This lower chargeability might be related to lower metal contents.

The cluster n°2 (in green) is characterized by higher chargeability possibly related to metal contents. This cluster could be related to higher metallic contents parts of the slag.

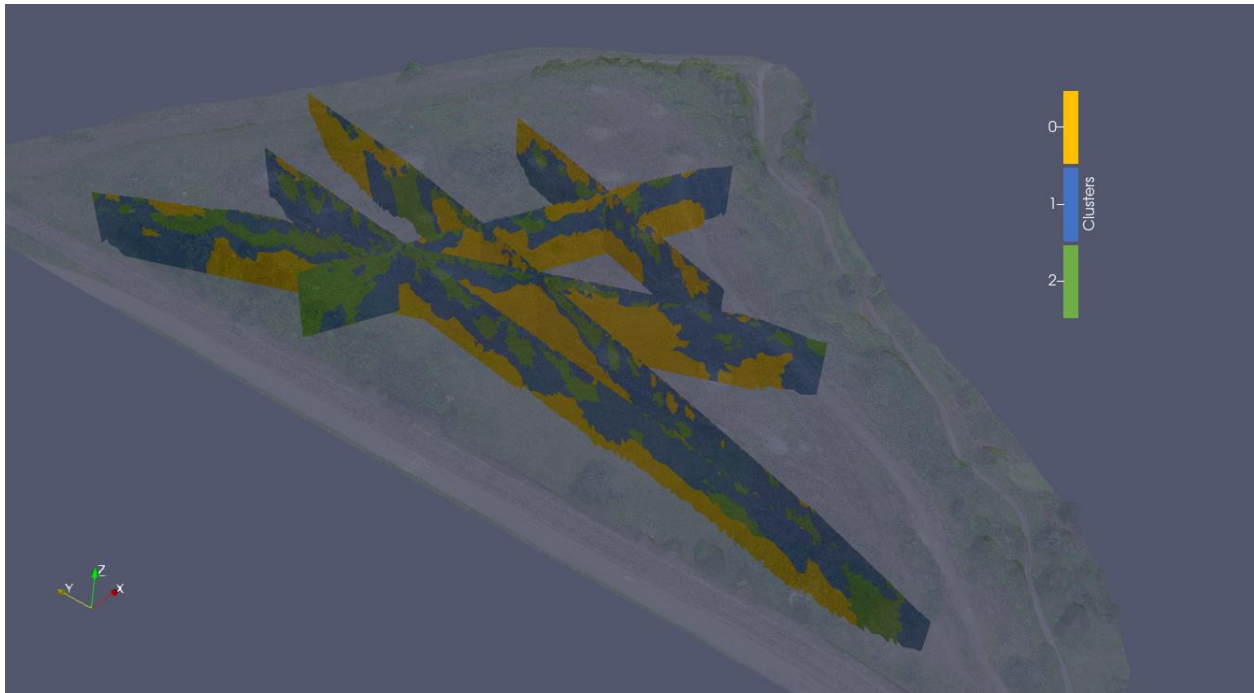


Figure 5: 3D view of the 3 geophysical clusters on the 5 profiles covered by the digital surface model.

These results and interpretations must be interpreted according to the current limit of the RADM. The geophysical imagery have not been compared with reliable ground truth. For that, we needed core drills from several place in the site to validate the interpretation. Without this, all the interpretation of geophysical properties is hypothetical. These interpretations rely on the experience glean during the project. The highly heterogeneous nature of the Teesside site does not allow direct transfer from another field site slag heap interpretation. In addition, the clustering of geophysical data is powerful, but has limits when it does not include other datasets. Finally, the imagery on only 2D profiles limits the estimation of volumes. A first estimation has been done in report DI1.3.1.

3. Investment site n°2: Pompey (Fr)

3.1. Pompey site presentation

Site description

The Pompey site is a former tailing pond from the iron and steel complex of Pompey-Frouard-Custines, located 10 km North from Nancy. The steel complex was active from 1870 to 1986. It is renowned for producing cast iron and special steels, such as ferromanganese (ferro-alloy rich in manganese). The last blast furnace of the Pompey-Frouard-Custines iron and steel complex was stopped in 1986. Over time, a forest ecosystem developed on the former tailing pond.

The geological substratum of the former tailing pond consists of the Lias marl formations (at 181 m NGF), which are covered by alluvium from the two rivers, composed of coarse siliceous materials (sands, gravel and pebbles) at the base over 3 to 6 m surmounted by finer materials (sands, silts and clays) on 1 to 3 m. These alluvial formations were locally exploited and backfilled with waste rock and iron and steel by-products. The depth of the deposits in the basin is estimated at around 10 m. The surface of the former pond is estimated to 26 000 m², for a total estimated volume of wastes equal to 260 000 m³.

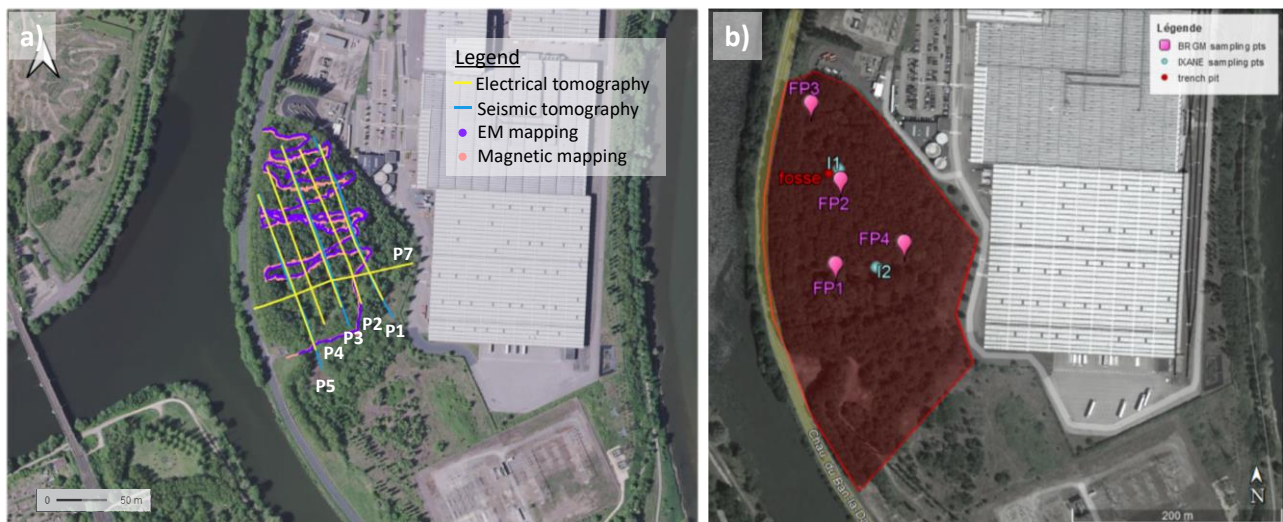


Figure 6 : Map of the Pompey site showing the location of: a) the different geophysical profiling or mapping measurements and b) the different sampling locations

Geophysical field acquisition

On-site work included a two-stage geophysical campaign and sampling campaign (see Figure 6).

Geophysical data on site were acquired at two different times: (1) a first electrical profile (P3 on Figure 6), completed by magnetic susceptibility measurements in the trench pit were conducted in November 2020; (2) Measurements on 5 electrical profiles (P1 to P7), 3 seismic

profiles (P1, P3 and P5), an electromagnetic map and a magnetic map were led in March 2021 (see Figure 6). More detailed information on the data acquisition and data processing can be found in the site-specific reports of geophysical investigation plan and survey, deliverables DI2.1.2 and DI2.2.1.

The ERT and IP results gave the most interesting and detailed information on the structure of the site. These results were used to set the position of the boreholes dug during the targeted sampling (see Figure 7). The choice of the location of each boreholes is discussed in details in deliverable DI2.2.1.

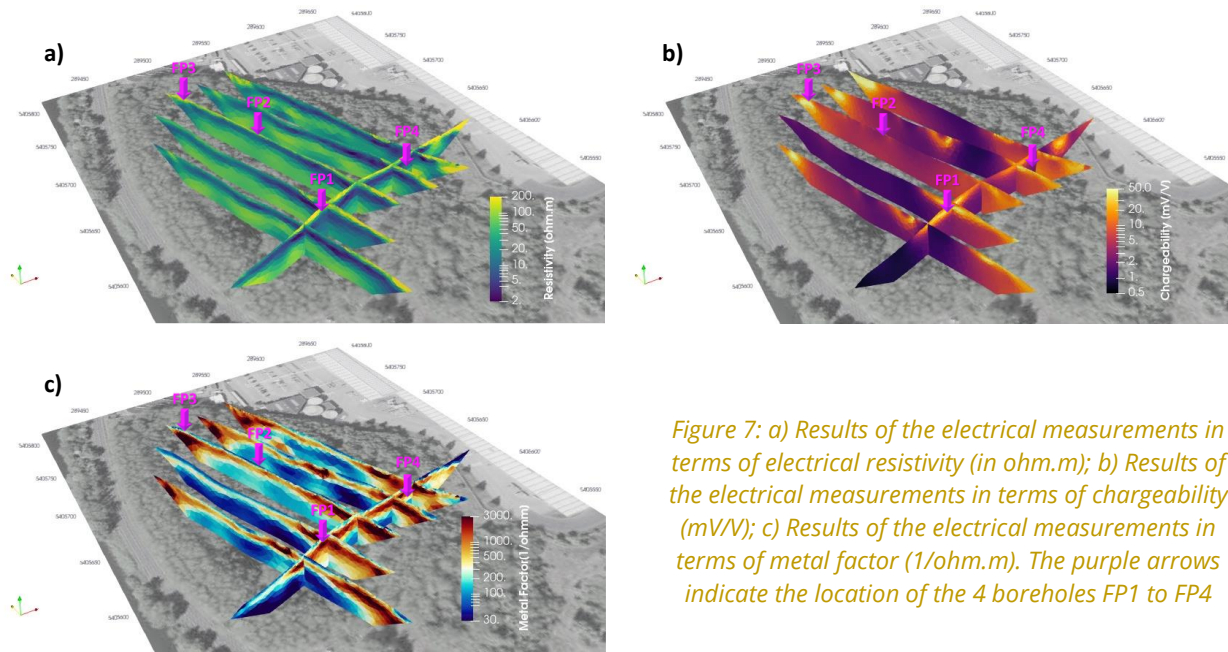


Figure 7: a) Results of the electrical measurements in terms of electrical resistivity (in ohm.m); b) Results of the electrical measurements in terms of chargeability (mV/V); c) Results of the electrical measurements in terms of metal factor (1/ohm.m). The purple arrows indicate the location of the 4 boreholes FP1 to FP4

In this report, we focus on ERT and IP to support further data processing to derive the raw material distribution model.

Targeted sampling

Two phases of sampling were handled on site: (1) traditional sampling prior to the geophysical investigations in fall 2020, within an already-existing pit, from 0 to 2 m deep; (2) targeted sampling after the geophysical investigations in the summer 2021 within 4 selected boreholes, from 0 to 9 m deep (see Figure 6 b) and Figure 7). Traditional sampling investigations on past metallurgical sites and deposits aims at characterizing the nature, physical and chemical composition of the wastes at a punctual location.

Geochemical laboratory analyses

During the targeted sampling, 45 samples were extracted from 4 different locations. A portable X-ray fluorescence spectrometer (pXRF) was used to analyze the chemical composition of all the samples. The concentration of 31 chemical elements was estimated including Fe, Mn, Zn, Cu and also other lighter metallic elements such as S ...

For a detailed description of the geochemical data measured in the lab, see the report on traditional sampling investigations DI2.1.2, and also the site-specific dataset for geophysical characterization (deliverable DI2.2.4). Additionally, the studies on the correlations between

the geochemical lab datasets together, and also with the geophysical field dataset can be found in the report corresponding to deliverable DI2.2.3.

3.2. Methodology for data interpretation

A similar methodology and data processing than for Investement site n°3 was used to interpret the geophysical field data and therefore, to derive the raw materials distribution model (see Figure 12). The 4 steps with their results are detailed in section 3.3.

3.3. Raw materials and pollution distribution model

Step 1: Creation of the field/lab dataset

In the first step of the methodology, we integrate the field geophysical data (collocated with the samples) and the geochemical lab measurements to carry out a multivariate statistical analysis (see deliverable DI2.2.3).

Step 2: Geostatistical identification of correlations

Two different statistical analysis were used to identify correlations between: (1) the chemical elements, and (2) the chemical elements and the geophysical parameters.

The first used was the Pearson's correlation coefficient analysis. It allows correlating variables 2-by-2. It is interesting because it shows positive and negative correlations. However, it is not very well suited to analyze datasets with a lot of different variables, such as our dataset (31 variables for the chemical elements alone).

The second one used was the principal components analysis (PCA). It presents the advantage of reducing the number of dimensions considered in the correlation analysis. It allows identifying clusters both for the variables (= chemical elements and geophysical parameters) projected on the new calculated dimensions (principal components or PCs), and for the individuals (= samples).

Using PCA to link the geophysical parameters to specific chemical elements was not successful. Indeed, the geophysical parameters contributed to independent PCs. We tried to compare geophysical field data to laboratory geochemical analysis. The lack of correlation might come from an upscaling/downscaling bias.

We thus decided to use the PCA analysis on the chemical elements alone to distinguish layers with various compositions, and link these layers to geophysical parameters variations.

Step 3: Definition of clusters

Using the PCA on the 31 chemical elements studied, we were able to identify cluster of variables correlated with each other. We splitted the variables into 3 different clusters depending on their contributions to the calculated PCs. We then linked these clusters with groups identified within the individual analysis: group A corresponding to samples taken at the lowest altitudes, and group B corresponding to samples taken at medium altitudes, within the settling pond. Utterly, the geochemical dataset could be splitted into 4 clusters.

Their interpretation in terms of chemical composition, corresponding geophysical parameters variations and final interpretation can be found in Table 1.

Table 1: Summary of the observations made for each layers of materials, based on the cluster selection

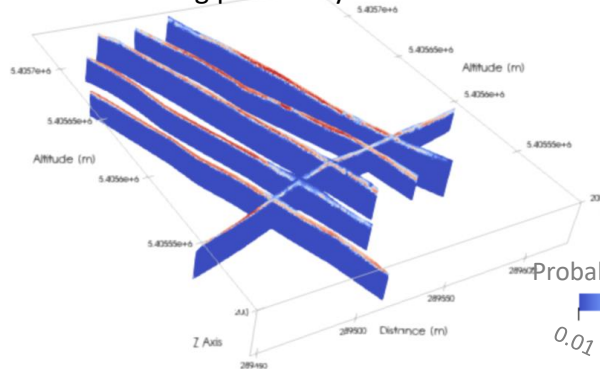
Altitudes [m]	Cluster n°	Chemical composition	Geophysical parameter variations	Interpretation
200 – 196	4	scattered	<ul style="list-style-type: none"> - High rho - Average M - Low MF 	Anthropic wastes placed after the closure of the settling pond
198 – 194	1	Main contributions: Zn, Cu and Pb, Mn	Transition zone: <ul style="list-style-type: none"> - Decrease of rho - Scattered M - Increase of MF 	Settling pond layer n°2
195 – 191	2	Main contribution: Fe	<ul style="list-style-type: none"> - Low rho - Scattered M - High MF 	Settling pond layer n°1
191 – 187	3	Main contributions: Si and K	<ul style="list-style-type: none"> - Low rho (slightly increasing) - Scattered M (decreasing) - High MF (slightly decreasing) 	Natural alluvia with high ionic strength electrolyte?

Step 4: field scale probabilistic classification

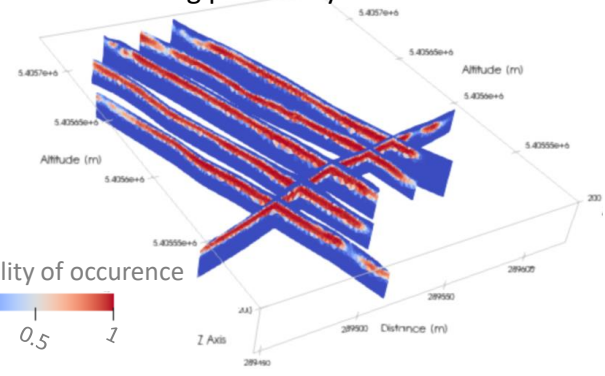
Based on the previously defined clusters at the borehole locations, we carried out a probabilistic classification of the field data (inverted models of resistivity and chargeability). Details on the probabilistic approach used can be found in part 4.2.

The results of step 4 are shown in Figure 8, where the probabilistic classification and the associated probability of occurrence for each cluster are presented. A high probability of occurrence is represented in red and a low probability in blue. For each cells of each profile, we then attribute a cluster number, corresponding to the maximum probability of occurrence.

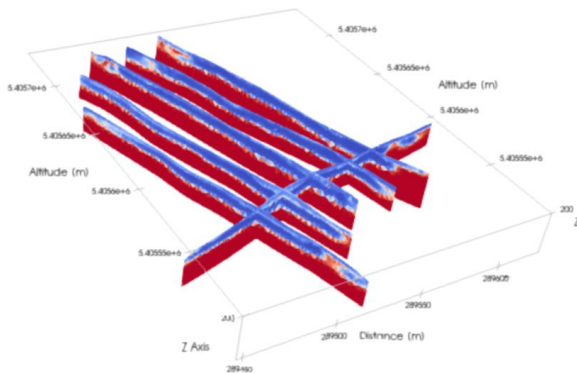
Cluster 1: settling pond – layer n°2



Cluster 2: settling pond – layer n°1



Cluster 3: natural alluvia



Cluster 4: Anthropic wastes

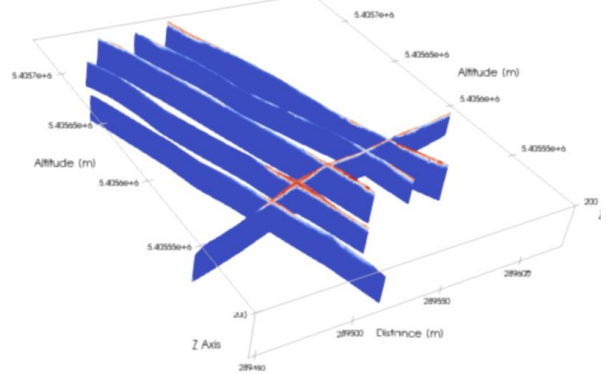


Figure 8 : Probability of occurrence of the 4 clusters estimated in step 3

Figure 9 defines the raw materials distribution model for the Pompey site. Most of the material correspond to cluster 3, which is the natural alluvia in which the settling pond was installed. Two layers corresponding to the settling pond material were identified (cluster n°1 and 2). The lateral north and south boundaries of these layers could be determined qualitatively with the electrical resistivity results. They are not as well defined with the geostatistical analysis. However, their vertical limit can be very well identified in Figure 9. Cluster n°4 corresponds to a layer of anthropic wastes. Their localization in Figure 9 corresponds to topographic heights, which is very realistic.

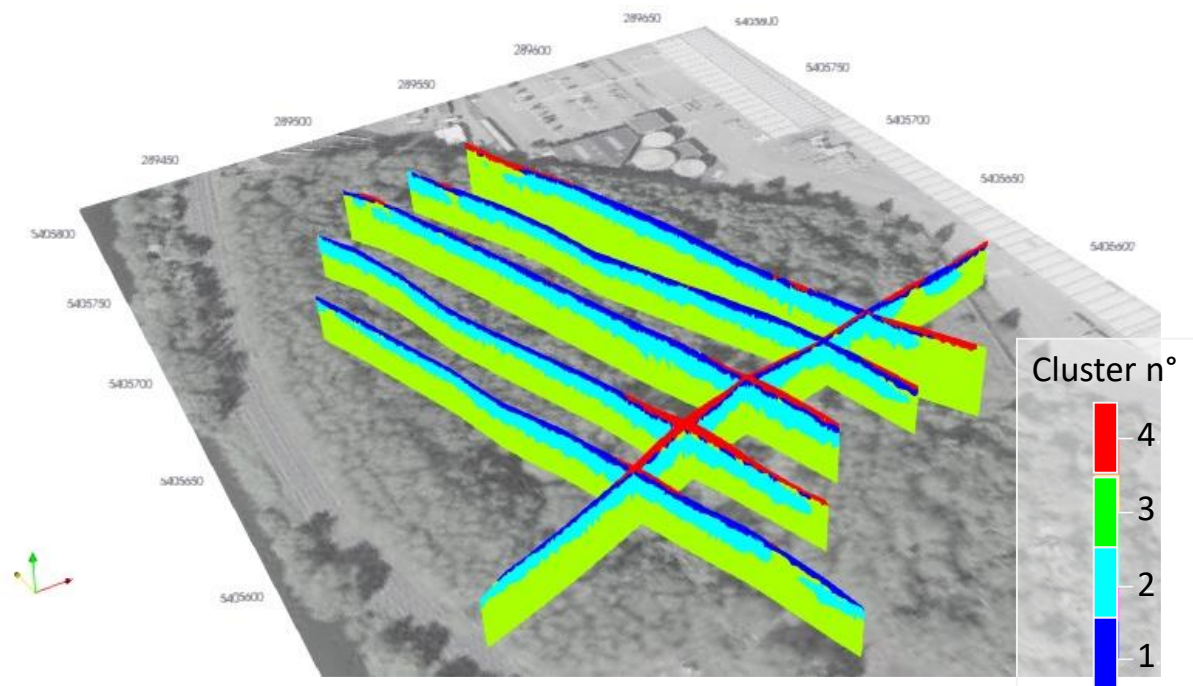


Figure 9 : Maximum of probability for each of the 4 clusters estimated in step 3

Because the geophysical measurements are only 2D, an estimation of the volumes for each cluster would need to interpolate the layers over the entire studied area. This result couldn't be achieved during this study, but would be interesting to go further in the quantitative approach. Laboratory geophysical dataset as well as mineralogical analysis would also be a good addition to go further in the recovery potential of the Pompey site.

4. Investment site n°3: Dufenco (Be)

4.1. Dufenco site presentation

Site description

The site of Dufenco – La Louvière (Wallonia, Belgium) is a former iron factory whose activities date back to 1850 and production of steel was carried out until the end of the 20th century. The factory is composed of several zones (see Fig. 10) where different activities were developed, e.g., coking plant, blast furnaces and tailings. In this contribution we focused on the slag heap, which according to the historical studies it is mainly composed of raw materials and by-products of the iron/steel making activities although heterogeneous waste is likely to be present (e.g., scrap metal, wood, refractories). More information can be found in the site-specific report that summarizes all available historical data, deliverable DI3.1.1.

In terms of geology, most of the slag heap is underlain by alluvium from the Thiriau stream. These quaternary deposits, which can be up to 8 to 10 meters thick, are composed of alternating sandy and clayey layers with local gravel content. Parts of the slag heap may also lie on the Houiller formation made of shale, sandstone and coal.

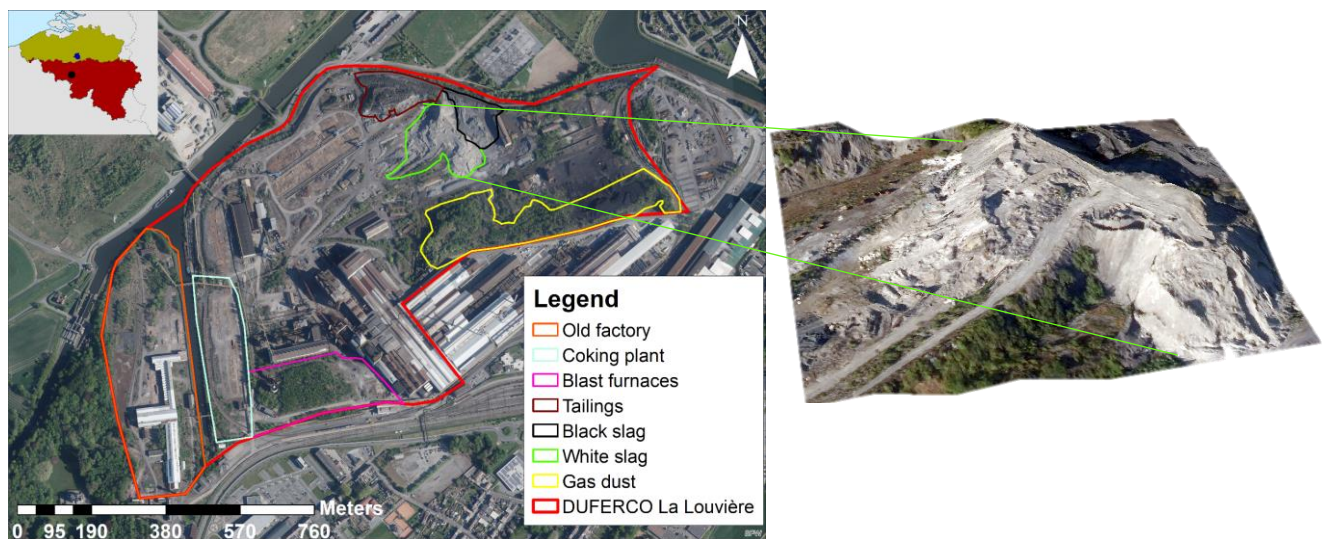


Figure 10: Aerial view of the Dufenco site with the delimitation of several activity zones. In this contribution we focused on the slag heap delineated in green solid lines.

Geophysical field acquisition and targeted sampling

We investigated the slag heap using time-domain electrical resistivity tomography (ERT) and induced polarization (IP) methods. Data were acquired with a Terrameter LS system from ABEM. In the white slag heap, 4 2D profiles were deployed, each containing 64 stainless steel electrodes spaced by 2 m. Data acquisition was carried out simultaneously on combinations of two profiles and inline and crossline measurements were collected to obtain a 3D model. More detailed information on the data acquisition and data processing can be found in the

site-specific reports of geophysical investigation plan and survey, deliverables DI3.1.2 and DI3.2.

Based on the geophysical results, we designed a sampling survey composed of pits excavations at 8 locations in the slag heap and within the geophysical acquisition domain, and samples were taken at depths of 1, 3 and 5 m.

Figure 11 shows the final 3D resistivity and chargeability models together with the electrodes position and sampling location. We use the relative cumulative sensitivity to assess the inverted models, e.g., Caterina et al. (2013). In general, the sensitivity of an inverted model decreases with depth. The cross-sections presented in Figure 11 include a sensitivity threshold to clip out model cells that might not be reliable.

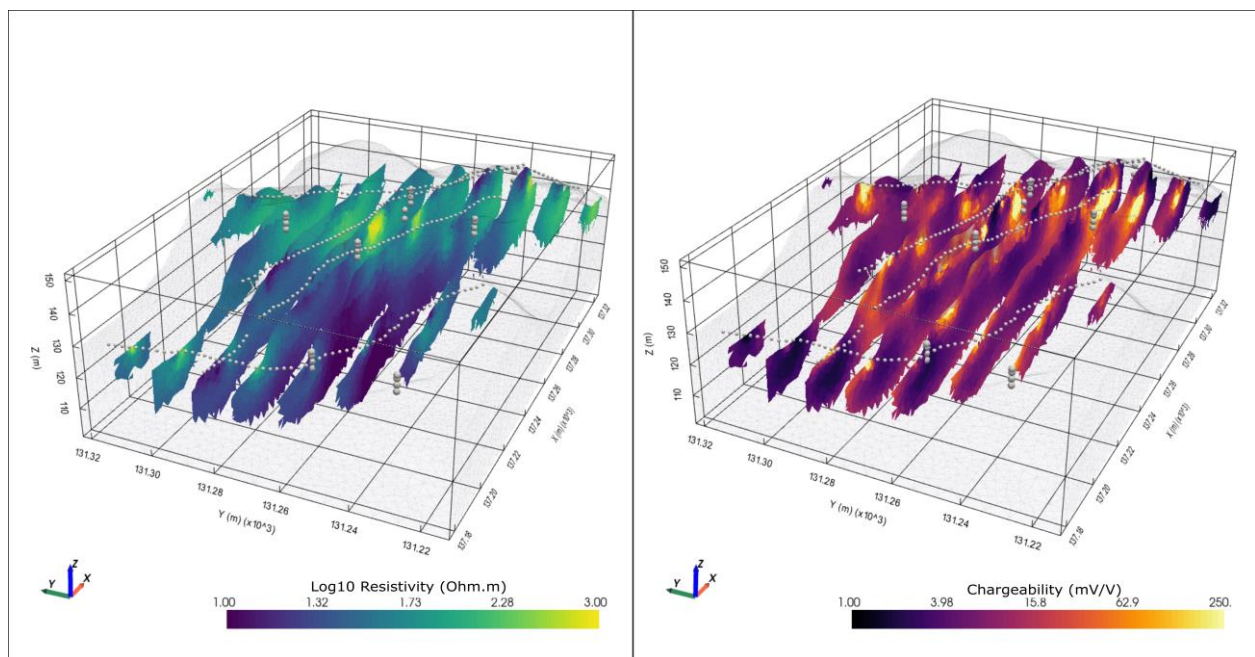


Figure 11: 3D resistivity and chargeability models shown as several cross-sections around the Y axis. The electrodes used in the acquisition are shown on the ground surface of the heap as small dots. Large spheres represent the location of the samples.

Geophysical laboratory measurements and geochemical analyses

We used the geophysical methods of time-domain ERT and IP as well as spectral induced polarization (SIP). In this report, we focus on ERT and IP to support further data processing to derive the raw material distribution model.

Resistivity and chargeability measurements were carried out in all the samples using columns of 1.5 dm^3 ($0.08 \text{ m } \varnothing \times 0.3 \text{ m}$) using a Terrameter LS system from ABEM using 4 electrodes similar to a Wenner array. Electrical current was injected for 2 s (delay of 0.8 s and acquisition of 1.2 s) and the voltage decay was measured during 1.86 s after the current was switched off. Geochemical investigations were conducted in the same set of samples. The samples were studied through X-ray fluorescence (XRF) analyses of major elements such as Fe, Mg, Al and Zn. Measurements of particle size distribution were also carried out.

For a detailed description of the geophysical data measured in the lab, see the report on site-specific dataset for geophysical characterization, deliverable DI3.2.4. Additionally, the studies on the correlations between the geochemical and geophysical lab data can be found in the report corresponding to deliverable DI3.2.3.

4.2. Methodology for data interpretation

In this subsection, we describe the methodology and data processing we used to interpret the geophysical field data and therefore, to derive the raw materials distribution model, see Figure 12.

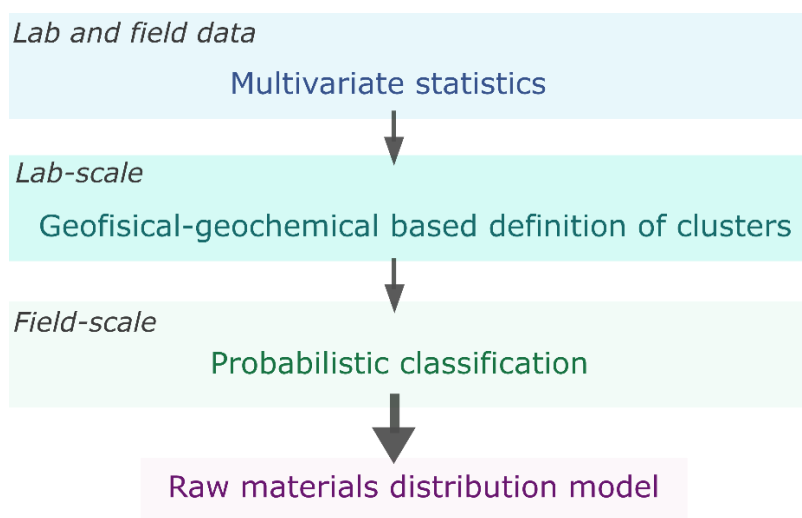


Figure 12. Methodology to derive the raw materials distribution model. In each step we indicate whether the data is from laboratory or field measurements or both.

In the first step of the methodology, we integrate the laboratory and field geophysical data (collocated with the samples¹) and the geochemical lab measurements to carry out a multivariate statistical analysis (see deliverable DI3.2.3). We study linear correlations between pairs of previously standardized data using the average content of chemical elements constituting all the samples and the geophysical variables measured in the lab and in the field, i.e., chargeability, resistivity (or its inverse the electrical conductivity).

As we identified that both chargeability and the electrical conductivity were able to resolve variations of Fe, Mn and Si (which were the elements of interest with higher concentrations), we focused on these variables (lab data) in the second step. The objective of the second step is therefore to identify groups of samples with different chemical composition and geophysical signatures.

¹ The geophysical field data collocated with the samples were derived from the average of the cells from the inverted models computed within a volume of dimensions 3 m × 3 m × 1.6 m centered at the positions where the samples were collected.

Lastly, based on the previously defined clusters or groups, we carried out a probabilistic classification of the field data (inverted models of resistivity and chargeability). To this aim, we first fitted the resistivity and chargeability field data (collocated with the samples) using a 2d kernel density estimator function for each group. Then we computed the joint conditional probabilities in the whole field acquisition domain for each group. We then compared these probability values and selected the group corresponding to the largest probability to classify the whole field data in terms of the different groups, i.e., raw materials and distribution model. Therefore, in addition to the classification model we also have the model with associated probability values or a measure of the classification uncertainty.

4.3. Raw materials distribution model

Figure 13 presents the results of step 2 of the former methodology. It presents the cross-plots of the chargeability (C_{lab}) vs the conductivity (σ_{lab}) values measured in the laboratory for all the samples. The colorbar represents the average concentrations of Mn, Fe and Si (from left to right). We also show the identified geophysical-geochemical based groups of samples, illustrating them in the cross-plot with the average concentration of Mn, but detailed grouping is described in Table 2. Note that we based the probabilistic classification in terms of the groups or clusters identified here.

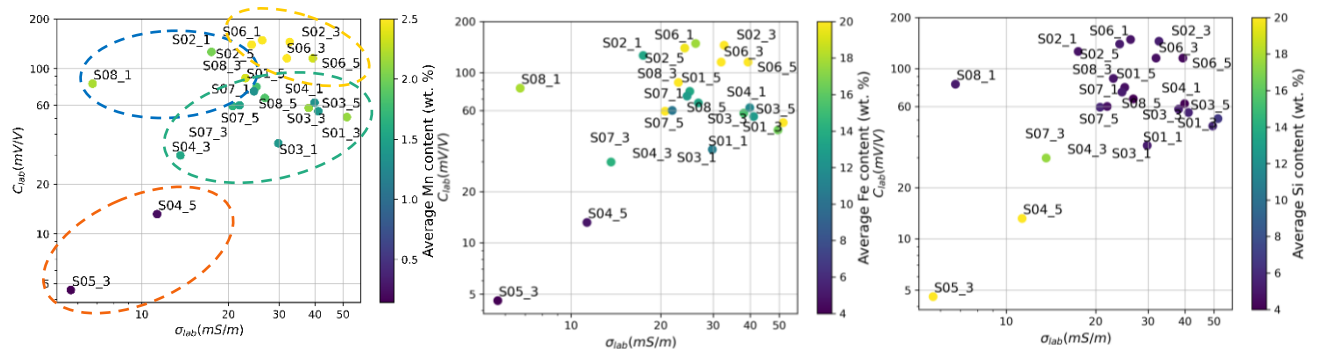


Figure 13. Cross-plots of the chargeability vs the conductivity (inverse of the resistivity) measured in the laboratory. Colorbars represent, from left to right, the average content of Mn, Fe and Si.

Table 2 describes the samples that correspond to each group, as well as a value range of conductivity values (inverse of resistivity) and a value range of chargeability values. We also describe what are the dominant elements that could be of potential interest for recovery in each group. Finally, we include a column with the amount of metallic content per group (mostly dominated by Fe and Mn).

The results of step 3 are shown in Figure 14 where the probabilistic classification and the associated probability values are presented. The models show several sections across the Y and X axis but they are 3D models covering most of the slag heap.

Table 2. Samples identified in each group from chemical analysis and geophysical-lab measurements.

Group identifier	Samples	σ_{lab}	C_{lab}	Group composition	Metallic concentration ²
Group 1	S04_5, S05_3	< 20 mS/m	< 20 mV/V	Si-Ti-K	Low
Group 2	S02_3, S02_5, S06_1, S06_3, S06_5	> 20 mS/m	> 100 mV/V	Fe-Mn-V-Cr	High
Group 3	S01_1, S01_3, S01_5, S03_1, S03_3, S03_5, S04_1, S04_3, S07_1, S07_3, S07_5, S08_5	> 14 mV/V	< 90 mV/V > 20 mV/V	Fe-Mn-V-Cr	Low-intermediate
Group 4	S02_1, S08_1, S08_3	< 25 mS/m	> 70 mV/V	Fe-Mn-V-Cr	Intermediate-large

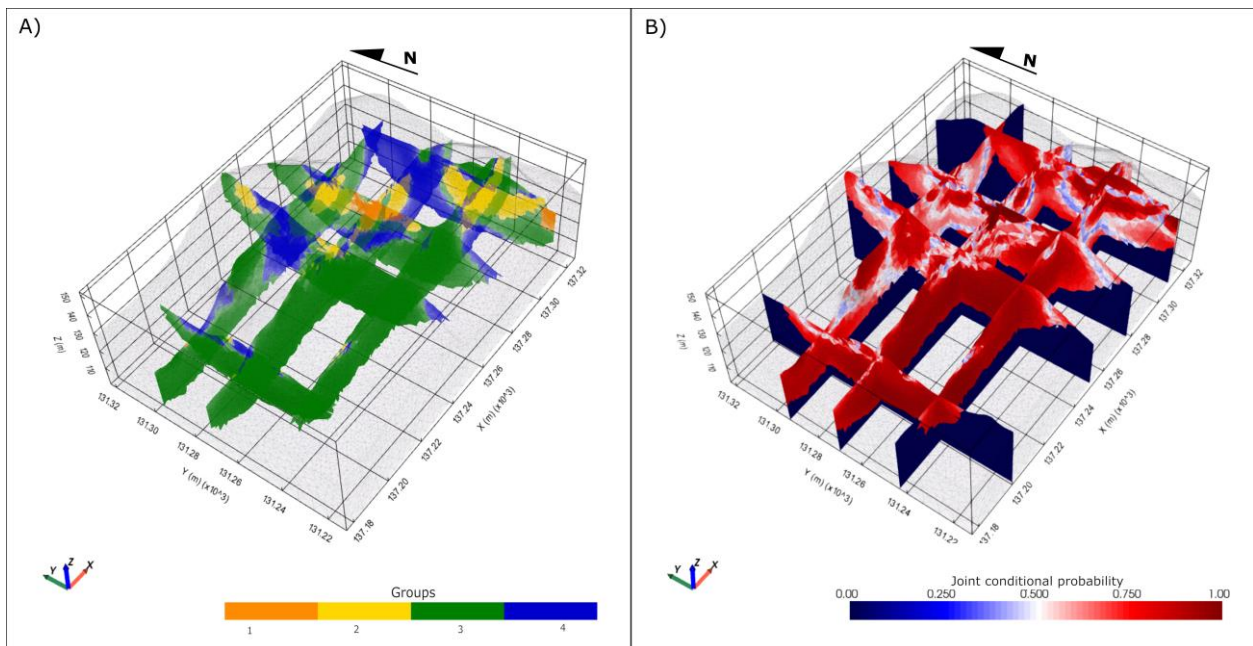


Figure 14. A) Classification of the field data and associated B) joint conditional probability. Transparency along the sections represent the resulting probability values. Both images integrate the sensitivity threshold ($>10^{-5.5}$).

Figure 14 defines the raw materials distribution model, where most of the material correspond to Group 3 while the materials corresponding to Group 2 represent the smallest

² Largely based on Mn and Fe.

proportion of the slags. Based on this model we also estimate the volumes of each group, the results are shown in Figure 15. The estimated volumes for Groups 1-4 are respectively: $4000 \text{ m}^3 \pm 12\%$, $23\,000 \text{ m}^3 \pm 21\%$, $189\,000 \text{ m}^3 \pm 12\%$ and $59\,400 \text{ m}^3 \pm 19\%$. The uncertainty ranges are derived from including the resulting probability values of the classification, i.e., volumes are estimated considering the probabilities (weighted volumes) and not considering the probabilities, then both estimations are compared.

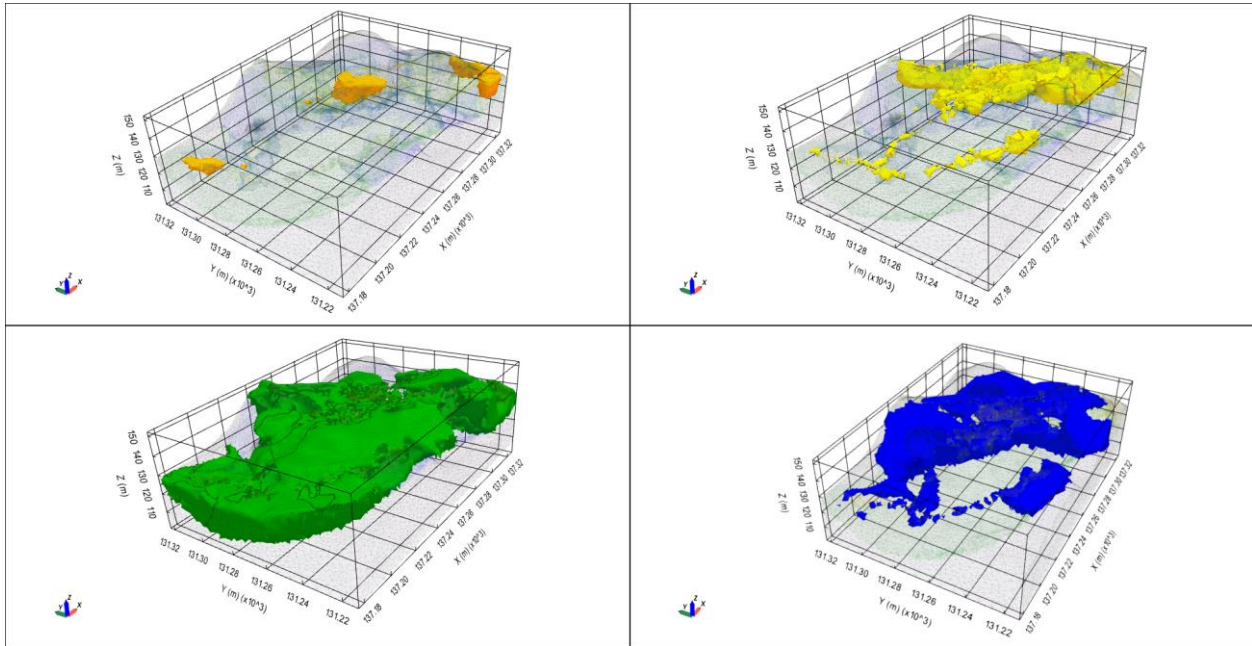


Figure 15. Volumes of each group.

Group 1 presents the smallest volume of material and according to its composition, it has the smallest metallic concentration. This group may be largely composed of inert waste. The materials of Group 2 present the largest metallic concentration, and it represents the most interesting volume for potential recovery. The volume of Group 3 represents most of the material of the slag heap and the materials are distributed across the entire volume of the heap. Lastly the materials of Group 4 are largely distributed towards the east of the heap and although the properties of this group are very similar to group 3, there is a larger concentration of Mn in group 4.

Preliminary conclusions

The use of a probabilistic classification of the field data allows to derive a raw materials distribution model that includes the uncertainty of the data interpretation and it is able to integrate this uncertainty in the estimation of volumes. This can be useful information to assess potential of resource recovery and for the management of the site in general. Note that this methodology can be adapted to conduct interpretations of field data in terms of more detailed or specialized chemical studies, e.g., mineralogical analysis.

5. General conclusions

This report illustrates three different approaches that can be followed to derive a more quantitative interpretation of geophysical data measured in the field through RADM models. These are conceptual models represented in terms of materials of interest, different chemical composition, metallic content, etc. The approaches showed here were adapted according to site-specific conditions, geophysical methods applied in the site and available sampling. As illustrated with the first site, when sampling within the deposits is not available, an approach of unsupervised learning can be conducted, i.e., clustering. This allows to identify groups or clusters in the field data with different geophysical properties that could be indicators of materials of different geochemical composition. On the other hand, when excavations are conducted through trial pits or boreholes and sampling can be carried out at larger depths, geophysical and geochemical measurements can also be made in the samples. In this case the objective is to calibrate the geophysical data (either from the lab or from the field) with the geochemical measurements. This calibration can be extrapolated into the whole model domain of the field data as illustrated with the approaches presented for pilot sites two and three. The latter approaches are based on a probabilistic classification of the field data, that allows to include the uncertainty in the interpretation and in the subsequent volume estimation. In general, geophysical imaging represents a suitable tool to derive raw material distribution models in PMSD and estimate volumes. Yet, to mitigate the ambiguity that geophysical surface methods may pose, calibration with ground truth data is needed.